Journal of the Korea Academia-Industrial cooperation Society
Vol. 19, No. 3 pp. 584-593, 2018

https://doi.org/10.5762/KAIS.2018.19.3.584
ISSN 1975-4701 / eISSN 2288-4688

Performance of Adaptive Maximum Torque Per Amp Control at Multiple Operating Points for Induction Motor Drives

Chun-Ki Kwon*, Yong-Hae Kong

Department of Medical IT Engineering, Soonchunhyang University

유도전동기 드라이브에서의 단위전류당 최대토크적응 제어기의 다운전점에서의 성능 연구

권춘기*, 공용해

순천향대학교 의료IT공학과

Abstract The highly efficient operation of induction motors has been studied in the past years. Among the many attempts made to obtain highly efficient operation, Maximum Torque Per Amp (MTPA) controls in induction motor drives were proposed. This method enables induction motor drives to operate very efficiently since it achieves the desired torque with the minimal stator current. This is because the alternate qd induction motor model (AQDM) is a highly accurate mathematical model to represent the dynamic characteristics of induction motors. However, it has been shown that the variation of the rotor resistance degrades the performance of the MTPA control significantly, thus leading to its failure to satisfy the maximum torque per amp condition. To take into consideration the mismatch between the actual value of the rotor resistance and its parameter value in the design of the control strategy, an adaptive MTPA control was proposed. In this work, this adaptive MTPA control is investigated in order to achieve the desired torque with the minimum stator current at multiple operating points. The experimental study showed that (i) the desired torque was accurately achieved even though there was a deviation of the order of 5% from the commanded torque value at a torque reference of 25 Nm (tracking performance), and (ii) the minimum stator current for the desired torque (maximum torque per amp condition) was consistently satisfied at multiple operating points, as the rotor temperature increased.

요 약 유도전동기를 고효율로 제어하기 위한 다양한 연구가 진행되어 왔다. 그 중에서 단위전류당 최대토크 제어기는 최소한의 고정자 전류로 원하는 토크를 제공하기 때문에 유도전동기 드라이브에서 고효율의 동작을 제공한다. 이는 유도전동기를 수학적으로 정밀하게 표현하는 대안모델을 기반으로 제어기가 설계되었기 때문이다. 그러나, 온도 변화에 따른 회전자 저항의 변이는 대안모델의 파라미터와 실제의 유도전동기의 파라미터의 불일치가 발생하여 단위전류당 최대토크 성능을 심각하게 저해하고 단위전류당 최대토크 제어 조건을 만족하지 못하게 하게 있다. 이러한 유도전동기의 운전시에 발생하는 열적 상승으로 인한 파라미터 값의 변화를 고려하는 단위전류당 최대토크적응 제어기가 제안되었다. 본 논문에서는 단위전류당 최대토크적응 제어기가 다수의 운전영역에서도 최소의 고정자 전류로 원하는 토크를 성취하는지를 검토하였다. 실험을 통한 연구에서 회전자의 온도가 증가하더라도 다수의 운전영역에서 25Nm의 토크 명령에서 5%의 차이가 존재하더라도 토크 명령을 정확하게 추구하고 또한, 원하는 토크를 최소한의 고정자 전류로 얻어짐을 확인함으로써 단위전류당 최대토크적응 제어기의 우수성을 검증하였다.

Keywords : Induction motor model, maximum torque per amp (MTPA) control, maximum torque per amp condition, multiple operating points, rotor resistance variation, thermal effects

This work was supported in part by the National Research Foundation of Korea(NRF) grant funded by the Korea government (Ministry of Science and ICT) (no. 2017R1D1A1B03029844)

*Corresponding Author : Chun-Ki Kwon(Soonchunhyang Univ.)
Tel: +82-41-530-3091 email: chunkikwon@sch.ac.kr

Received January 2, 2018 Revised February 14, 2018
Accepted March 9, 2018 Published March 31, 2018

1. Introduction

Highly efficient operation of induction motor has been studied in the past years [1-9]. Among many efforts to obtain highly efficient operation, Maximum Torque Per Amp (MTPA) controls in induction motor drives were proposed [8][9]. Therein, the MTPA control based on an alternate *qd* induction machine model (AQDM) [8] outperformed MTPA control strategy based on the classical *qd* model (CQDM) such as in [9]. This (AQDM) is highly accurate mathematical model to represent dynamic characteristics of induction motors [10]. The MTPA control proposed in [8] has been shown to achieve the commanded torque with good accuracy; it has also been shown that the maximum torque per amp condition is, in fact, satisfied at which condition the produced torque is always largest for a given stator current

However, performance of control strategy can be degraded significantly due to the mismatch between the actual value of rotor resistance and its parameter value in the design of control strategy as rotor temperature varies. Thus, the consideration has been a significant issue in control design, particularly in the case of highly efficient controls [11-18]. To overcome degradation in performance of MTPA control in [8] as rotor temperature varies during operation, Adaptive MTPA control strategy was proposed to take rotor resistance variation into account. Consequently, the performance of adaptive MTPA control strategy was validated to achieve torque command with minimal stator current. However, this study was carried out at rated operating point, which is 150 Nm..

In this work, the adaptive MTPA control strategy is investigated at multiple operating points. In the adaptive MTPA control strategy, rotor resistance estimate is added as one of input variables in the existing MTPA control to take rotor resistance variation into account. Actual rotor resistance can be estimated using any on-line rotor resistance estimator available in the literature [11-18]. The Adaptive MTPA control is experimentally shown to obtain the desired torque with high accuracy (called tracking performance) and, at the same time, to satisfy the maximum torque for a given stator current (called maximum torque per amp condition), at multiple operating points.

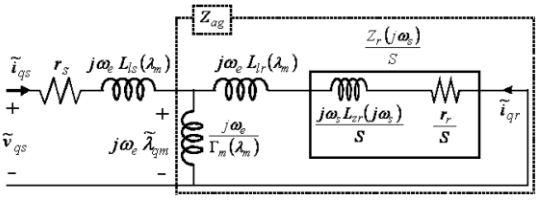

Fig. 1. Steady-state equivalent circuit of AQDM model with rotor impedance represented as $r_r + j\omega_s L_{zr}(j\omega_s)$

2. Alternate QD Induction Motor Model

Unlike CQDM having constant parameters in [1-7,9,11-18], Alternate QD Induction Machine Model (AQDM) simultaneously included saturations in leakage and magnetizing path, and distributed system effects in the rotor circuits. The steady-state equivalent circuit of AQDM having parameters in analytical form is shown in Fig.1. Therein, ω_s is defined as $\omega_e - \omega_r$ and slip S as $S = \frac{(\omega_e - \omega_r)}{\omega_e}$. Magnitude of magnetizing flux linkage, λ_m, is equal to $\sqrt{2}|\widetilde{\lambda_{qm}}|$. Stator and rotor leakage inductance, and the absolute inverse magnetizing inductance are denoted as $L_{ls}(\bullet)$, $L_{lr}(\bullet)$, and $\Gamma_m(\bullet)$, respectively. The rotor impedance is formulated as $Z_r(j\omega_s)$ in Laplace to represent distributed system effects in the rotor circuits, and is into a real and imaginary part, which are denoted r_r and $j\omega_s L_{zr}(j\omega_s)$, respectively. Note that the imaginary part, $j\omega_s L_{zr}(j\omega_s)$, is inductive reactance which clearly depends upon slip frequency ω_s due to skin effects in rotor circuits. Additional details on the AQDM and nomenclature are set forth in [8,10].

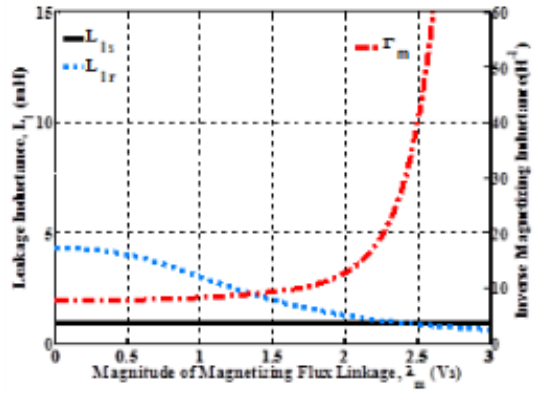

(a) Stator & rotor leakage inductances and inverse magnetizing inductance.

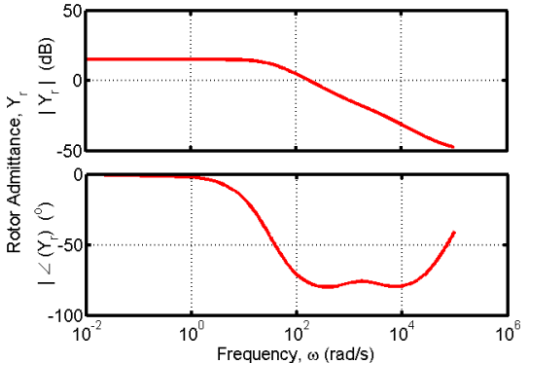

(b) rotor admittance

Fig. 2. AQDM parameters characterized for the test motor

To use AQDM for the design of control strategy, analytical forms should be selected in such a way that they not only represent magnetic characteristics accurately but do so with as few parameters as possible. Herein, the functional forms of (1) ~ (4) were used since AQDM model with (1) ~ (4) was found to give better fit to the measured impedance data taken from the test induction motor [8].

$$L_{ls} = l_{s1}(a\,constant) \tag{1}$$

$$L_{lr}(\lambda_m) = l_{r1} + \frac{l_{r2}}{1 + (l_{r3} \cdot \lambda_m)^{l_{r4}}} \tag{2}$$

$$\Gamma_m(\lambda_m) = m_1 - m_2 \cdot \lambda_m + e^{m_3(\lambda_m - m_4)} + e^{m_5(\lambda_m - m_6)} \tag{3}$$

$$Y_r(s = j\omega_s) = \frac{1}{Z_e(s = j\omega_s)} = \frac{y_{a1}}{y_{b1}s + 1} + \frac{y_{a2}}{y_{b2}s + 1} + \frac{y_{a3}}{y_{b3}s + 1} \tag{4}$$

The test induction motor used in this work is a 4-pole, 460V, 50Hp, 60Hz, delta-connected squirrel cage induction motor. The coefficients of (1) ~ (4) for AQDM were characterized using the parameter identification method in [8,10] as listed in Table 1 and shown in Fig. 2. The parameter identification for AQDM is omitted in this work because it is beyond the scope of this study. Its detailed procedure can be found in [8,10].

Table 1. Resultant Coefficients in Analytic Forms of (1) ~ (4)

(1) $L_{ls}(\cdot)$	(3) $\Gamma_m(\cdot)$	(4) $Y_r(\cdot)$
9.06e-4	6.79e 0	5.65e 0
(2) $L_{lr}(\cdot)$	6.62e-1	3.21e-2
1.40e-4	5.03e 0	4.40e-2
4.15e-3	1.85e 0	4.78e-4
7.35e-1	8.68e-1	3.17e-3
2.59e 0	1.29e-1	8.76e-8

3. AQDM Based Maximum Torque Per Amp Control Considering Rotor Resistance Variation

Based on analytical forms of (1) ~ (4) with their coefficients in Table 1, the Adaptive Maximum Torque Per Amp (Adaptive MTPA) control with rotor resistance variation taken into consideration is derived in this section for the highly efficient operation of induction motor even at light loads where Field Oriented Control (FOC) suffered from degrade in efficiency because the rated flux should be kept for a fast speed-of-response.

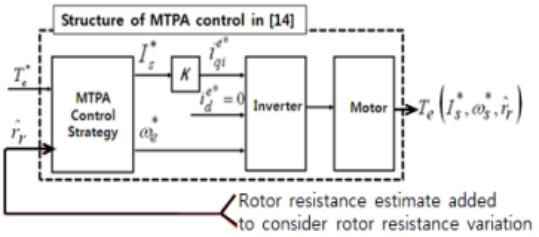

Fig. 3. Structure of the adaptive MTPA control with rotor resistance variation taken into account

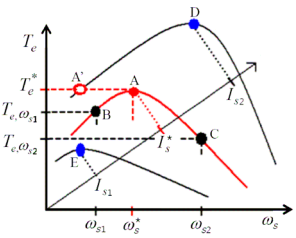

pts	Objective		Remark
	Te= Te*	MTPA Cond.	
A	O	O	· Te=Te* · Te : max for I_s^*
A'	O	X	· Te=Te* · Te : not max for I_{s2}
B	X	X	
C	X	X	
D	X	O	· Te≠Te* · Te : max for I_{s2}
E	X	O	· Te≠Te* · Te : max for I_{s1}

Fig. 4. The root-mean-square magnitude of the stator current I_s and slip frequency ω_s to achieve the objective of the maximum torque per amp control.

3.1 Structure

To take rotor resistance variation into consideration, rotor resistance estimate is added to an input of existing MTPA control in [8]. Thus, in the Adaptive MTPA control, root-mean-square magnitude of the stator current I_s and slip frequency ω_s are expressed not only as function of commanded torque, T_e^*, but also as function of rotor resistance estimate, $\hat{r}_r$.

3.2 Objective

The objective of the Adaptive MTPA control is to achieve following two properties, the tracking property and maximum torque per ampere (MTPA) condition regardless of rotor resistance variation as rotor temperature increases.

a. Tracking Property: The tracking property is to achieve the torque command.

$$\| T_e(\omega_s^*, I_s^*, \hat{r}_r) - T_e^* \| < \epsilon \qquad (5\text{-}1)$$

Herein, is a very small number. In Fig. 4, torque command T_e^* is achieved at operating point A and Point A'. Note that conduction loss is proportional to magnitude of stator current, thus more efficient operating in point A than in point A'.

b. Maximum Torque Per Amp (MTPA) Condition: MTPA condition is the condition at which the achieved torque $T_e^*(I_s^*, \omega_s^*, \hat{r}_r)$ should be maximum for a given stator current.

$$T_e(I_s^*, \omega_s^*, \hat{r}_r) = \underbrace{\max_{I_s, \omega_s}} T_e(I_s, \omega_s, \hat{r}_r) \qquad (5\text{-}2)$$

In Fig. 4, MTPA condition is satisfied at point A, point D, and point E for the stator current I_s^*, I_{s2}, and I_{s1}, respectively. Thus, the objective of the Adaptive MTPA control is achieved only at point A where desired torque, T_e^*, is achieved with minimum stator current, I_s^*, thus minimizing conduction loss.

3.3 Derivation of torque in terms of stator current, slip frequency, and rotor resistance

The derivation of Adaptive MTPA control adaptive to rotor resistance variation is exactly identical to that of MTPA control in [8] except addition of rotor resistance estimate, $\hat{r}_r$, to input variable. In [8], $\hat{r}_r$ was fixed to 0.176 Ω which is the rotor resistance value at a specific temperature (near 43 $^\circ C$) for the characterization procedure of the test induction motor.

For convenience purposes, general torque equation in the synchronous reference frame [19] is re-written as

$$T_e = \frac{3}{2}\frac{P}{2}\left(\lambda_{dm}^e i_{qs}^e - \lambda_{qm}^e i_{ds}^e\right) \qquad (6)$$

Using the relationship between variable '*x*' in the *q*-axis in the phasor representation, and variable '*x*' in the *q*- and *d*- axis in the synchronous reference frame [19], which is

$$\sqrt{2}\,\widetilde{x_{qs}} = x_{qs}^{e} - jx_{ds}^{e}, \tag{7}$$

the equation (6) can be expressed as

$$T_e = \frac{3}{2} P\, Imag\left(\overline{\widetilde{\lambda_{qm}}}\ \widetilde{I_{qs}}\right) \tag{8}$$

Since we focus on magnitude of stator current, phase reference can be selected such that all the stator current in the synchronous reference frame is in the q-axis. With this assumption, (7) reduces to

$$\sqrt{2}\, I_s = i_{qs}^{e} \tag{9}$$

where I_s is the magnitude of $\widetilde{i_{qs}}$.

With (9), the electromagnetic torque in (8) can be rewritten in terms of magnitude of stator current and magnetizing flux linkage phasor in the *q*-axis as

$$T_e = \frac{3}{2} P\, Imag\left(\overline{\widetilde{\lambda_{qm}}}\ \ I_s\right) \tag{10}$$

where the overbar '¯' indicates complex conjugate.

From the AQDM steady-state equivalent circuit in Fig. 1, $\widetilde{\lambda_{qm}}$ is expressed as

$$\widetilde{\lambda_{qm}}(\omega_s, I_s, r_r) = \frac{Z_{ag}(\lambda_m, \omega_s, r_r)}{j\omega_e}\, I_s \tag{11}$$

where Z_{ag} is the impedance in parallel with $j\omega_e / \Gamma_m(\lambda_m)$ and $j\omega_e L_{lr}(\lambda_m) + Z_r(j\omega_s)/S$, which is

$$Z_{ag}(\lambda_m, \omega_s, r_r) = \frac{j\omega_e}{\Gamma_m(\lambda_m) + \dfrac{j\omega_s}{j\omega_s L_{lr}(\lambda_m) + (r_r + j\omega_s L_{zr}(j\omega_s))}} \tag{12}$$

Thus, with substitution of (11) into (10), the final electromagnetic torque in terms of ω_s, I_s, and r_r can be expressed as

$$T_e(\omega_s, I_s, r_r) = \frac{3}{2} P\, Imag\left(\overline{\left(\frac{Z_{ag}(\lambda_m, \omega_s, r_r)}{j\omega_e}\, I_s\right)}\ I_s\right) \tag{13}$$

where $\lambda_m(\omega_s, I_s, r_r)$ can be computed as

$$|\omega_e \lambda_m| = \sqrt{2}\ |I_s \bullet Z_{ag}(\lambda_m, \omega_s, r_r)| \tag{14}$$

since $\lambda_m = \sqrt{2}\,|\widetilde{\lambda_{qm}}|$. Any useful nonlinear algebraic equation solver can be used to solve $\lambda_m(\omega_s, I_s, r_r)$ in (14) in the process to achieve the torque in (13) when I_s, ω_s, and r_r are given.

3.4 Derivation of AQDM based Adaptive MTPA Control

With the final electromagnetic torque expressed in terms of ω_s, I_s ,and r_r in (13), we can re-formulate derivation of AQDM based Adaptive MTPA control as optimization problem

$$T_{e,\max} = \underbrace{\max imize}_{\omega_s} \frac{3}{2} P\, Imag\left(\overline{\left(\frac{Z_{ag}(\lambda_m, \omega_s, r_r)}{j\omega_e}\, I_s\right)}\ I_s\right) \tag{15}$$

By applying any optimization technique, (15) can be solved to find the optimal slip frequency, ω_s^* and the resultant maximum torque $T_{e,\max}$ at ω_s^* for stator current I_s and rotor resistance r_r. Herein, Newton-Raphson method was utilized as optimization technique. Since I_s ranges from nearly 0A to the rated current and r_r is selected to vary from 0.01 Ω to 0.21 Ω, the j-th point of I_s and k-th point of $r_r$will be denoted $I_{s,j}^*$ and $r_{r,k}$, respectively. With this, the resulting optimum slip frequency and the

corresponding maximum value of torque for $I_{s,j}^*$ and $r_{r,k}$ will be denoted $\omega_{s,j,k}^*$ and $T_{e,\max,j,k}^*$. The optimal slip frequency $\omega_{s,j,k}^*$ can be obtained by solving (15) for all combination of $I_{s,j}^*$ and $r_{r,k}$. These resulting data points, $\{I_{s,j}^*,\ T_{e,\max,j,k}^*, r_{r,k}\}$ for stator current and $\{\omega_{s,j,k}^*,\ T_{e,\max,j,k}^*, r_{r,k}\}$ for slip frequency, are recorded for post data processing as depicted in Fig. 5. One interesting observation is that I_s is not a function of r_r while ω_s is a function of r_r.

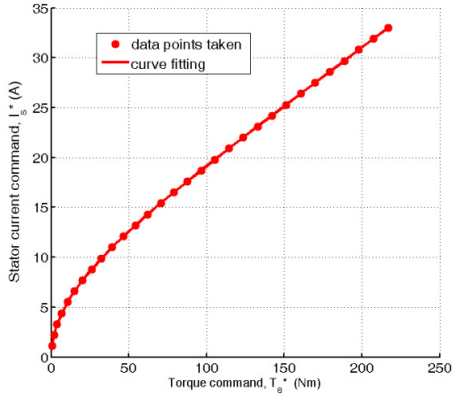

(a) Stator current command versus torque command

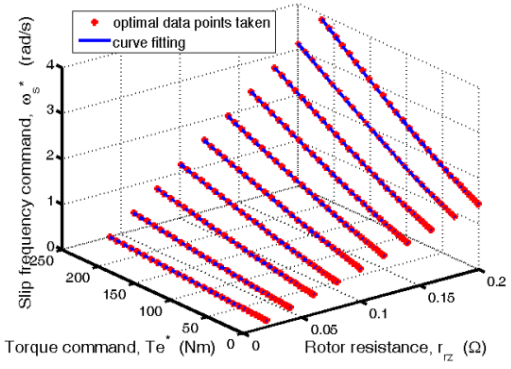

(b) Slip frequency command .vs. torque command and rotor resistance

Fig. 5. The control law and data points for the Adaptive MTPA control based on AQDM with different r_r

3.5 Curve fitting

The data points $\{I_{s,j}^*,\ T_{e,\max,j,k}^*, r_{r,k}\}$ and data points $\{\omega_{s,j,k}^*,\ T_{e,\max,j,k}^*, r_{r,k}\}$ in Fig. 5 are used to construct a stator current control law and slip frequency control law, respectively. For the stator current control law, the form to fit the data points $\{I_{s,j}^*,\ T_{e,\max,j,k}^*, r_{r,k}\}$ is assumed as

$$I_s^*(T_e^*) = a_1 T_e^* + a_2 T_e^{*b_1} + a_3 T_e^{*b_2} \tag{16}$$

Therein, a_1, a_2, a_3, b_1, and b_2 are obtained using a genetic algorithm, which was part of the Genetic Optimization System Engineering Tool (GOSET 1.02), a Matlab based toolbox in [20]. Any fitting technique could be used.

As for the slip frequency control law, the functional form to fit the data points $\{\omega_{s,j,k}^*,\ T_{e,\max,j,k}^*, r_{r,k}\}$ are formulated

$$\omega_{s,AMPTA}^*(T_e^*, r_r^*) = d_0 r_r^{*n1} + d_1 r_r^{*n2} T_e^{*n3} \tag{17}$$

where d_0, d_1, n_1, n_2, and n_3 are also identified by use of GOSET 1.02 toolbox.

The resulting control laws for I_s^* and ω_s^* for the test machine is obtained as follows

$$I_s^*(T_e^*) = 0.102\, T_e^* - 6.410\, T_e^{*0.011} + 7.790\, T_e^{*0.152} \tag{18}$$

$$\omega_{s,AMPTPA}^*(T_e^*, \hat{r_r}) = 7.22\, \hat{r_r}^{1.00} + 0.025 \hat{r_r}^{1.00}\, T_e^{*1.15} \tag{19}$$

In Fig. 5, it can be seen that (18) and (19) fit the recorded data points $\{I_{s,j}^*,\ T_{e,\max,j}^*\}$ and $\{\omega_{s,j,k}^*,\ T_{e,\max,j,k}^*, r_{r,k}\}$ in a good agreement, respectively.

4. Experimental Set-up

To help readers understand advantages from the MTPA control adaptive to rotor resistance variation, the performance degradation of MTPA control in [8], which

is not adaptive to rotor resistance variation, compared. Note that stator current, I_s, is identical in both control strategy because it is not a function of rotor resistance, r_r. Also, slip frequency, ω_s^*, control law in the MTPA control strategy in [8] can be obtained by substituting the value of 0.176 Ω for rotor resistance estimate, r_r, in (21) since 0.176 Ω is the value of the rotor resistance at the temperature of 43 ℃

$$\omega_{s,MTPA}^*\left(T_e^*\right) = 1.2707 + 0.0044\,T_e^{*\,1.15} \tag{20}$$

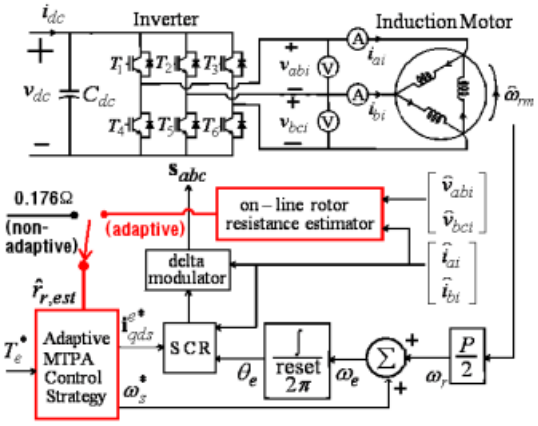

Fig. 6. The configuration of the Non-Adaptive and Adaptive MTPA control based induction machine drive

at which the test induction motor was characterized. For convenience purposes, the MTPA control in [8] is referred to as Non-Adaptive MTPA control in that slip frequency control law in (20) is not adaptive to rotor resistance variation, while the MTPA control adaptive to rotor resistance variation is referred to as Adaptive MTPA control since slip frequency control law in (19) is adaptive to rotor resistance variation.

For the study, a current controlled inverter-fed drive was used to operate the test induction motor. The configuration of the motor drive used in this study is depicted in Fig. 6. Therein, the upper part in Fig. 6 is the power converter topology. The lower part is composed of a speed control block with an anti-windup, Integrator, synchronous current regulator (SCR), and delta modulator, to determine the switching signal for switching devices, T_1~T_6. Additional details on the configuration for the drive and nomenclature are set forth in [9,19].

5. Performance of AMTPA Control at Multiple operating points with Rotor Resistance variation

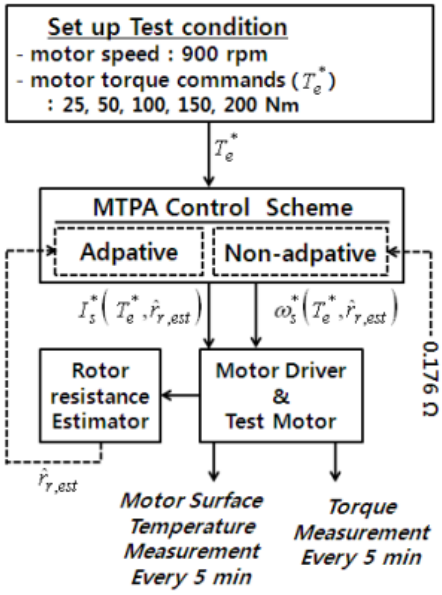

Fig. 7. Experimental flow chart

The performance of the Adaptive MTPA control strategy is compared with that of the Non-adaptive MTPA control strategy as rotor temperature varies at multiple operating points as shown in Fig. 7. With the experimental setup mentioned in Section 4, due to the difficulty in directly measuring the actual rotor resistance of the test motor, the rotor resistance estimator proposed in [13] was utilized and incorporated into the MTPA control.

In this study, five different torque commands are sequentially applied as the stator (and presumably rotor) temperature increases. The commanded torque is selected to test the control from light load to heavy

load. The sequence of torque commands is: 25 Nm, 50 Nm, 100 Nm, 150 Nm, and 200 Nm.

In Fig. 8, the torque produced by the Adaptive MTPA control strategy is compared to the torque generated by the Non-Adaptive MTPA control strategy during a sequence of different operating conditions. In Fig. 8 (a), the solid line indicates the torque estimate produced by the Adaptive MTPA control and the dashed line indicates the torque estimate by the Non-Adaptive MTPA control. Therein, the Adaptive MTPA control strategy outperforms the Non-Adaptive MTPA control strategy at operating conditions where the rotor resistance does not match the effective rotor resistance used to design the Non-Adaptive MTPA control law in (18) and (20).

Despite the improvements of the performance by the Adaptive MTPA control strategy over the Non-Adaptive MTPA control strategy, there exists deviation on the order of 5 % from the commanded torque in the case of the operation conditions where the torque commands are set to 25 Nm. This may be due to more significant current sensor error, poorer performance of the rotor resistance estimator, and less accuracy of AQDM, at low current levels. All of these factors contribute to the approximately 5 % error.

Two additional sets of torque estimates are shown in Fig. 8(b). They corresponds to the Non-Adaptive MTPA control strategy at 0.9 and 1.1 times of $\omega^*_{s,MTPA}$ in (20) of the Non-Adaptive MTPA control strategy at changing operating conditions have been included. Therein, as temperature increases, the value of slip frequency at which the most torque is produced by the Non-Adaptive MTPA control strategy varies. In the initial part of study, when the temperature is low and where rotor resistance is smaller than the rotor resistance used to design Non-Adaptive MTPA control strategy, the torque estimated at 0.9 times of $\omega^*_{s,MTPA}$ given by (20) is largest (of Non-adaptive MTPA control strategy). In the middle part (in time) of the study, when the rotor resistance was close to the design value, it can be seen that a slip value of $\omega_s = \omega^*_{s,MTPA}$ given by (20) yields the most torque (again, of Non-adaptive MTPA control strategy). Finally, as the studies proceed in time, eventually the largest torque estimate was obtained using 1.1 times $\omega^*_{s,MTPA}$ of Non-Adaptive MTPA control strategy. The Adaptive MTPA control strategy adjusts the slip frequency command, $\omega^*_{s,AMTPA}$, given by (19) such that maximum torque per amp condition is always achieved at multiple operating points.

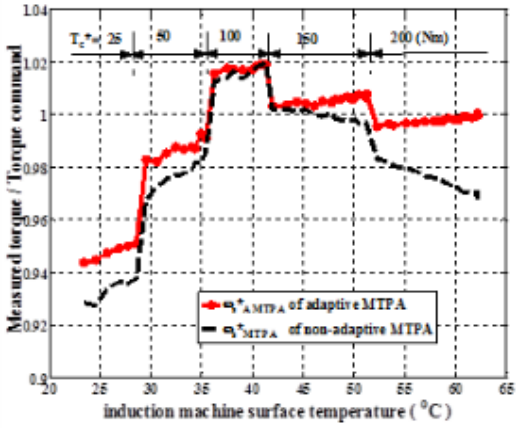

(a) Measured torque versus induction machine surface temperature

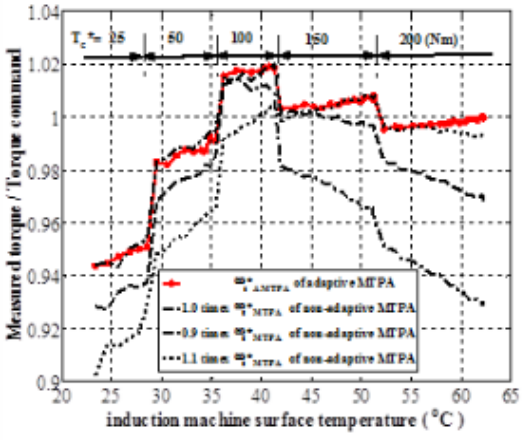

(b) Maximum torque per amp condition

Fig. 8. Comparisons of the performances by the static MTPA control strategy and the adaptive MTPA control strategy at several operating conditions from light load to heavy load

The observations from Fig. 8 indicate that the adaptive MTPA control strategy achieves the desired torque more accurately than the Non-Adaptive MTPA control strategy and satisfies maximum torque per amp condition regardless of changing operating points and rotor temperature variation. Furthermore, compared to the torque produced by the Non-Adaptive MTPA control strategy given by (18) and (20), the torque produced by the Adaptive MTPA control strategy given by (18) and (19) was not degraded by rotor temperature rise.

6. Conclusion

Experimental study shows that the Adaptive MTPA control at multiple operating points outperforms MTPA control. The Adaptive MTPA control is observed to achieve more accurate commanded torque and satisfying MTPA condition as rotor temperature increases even though there exists deviation on the order of 5 % from the commanded torque in the case of the light load operation conditions such as torque reference of 25 Nm.

This is because rotor resistance variation is taken into account, which makes slip frequency control law adaptive to rotor resistance variation. In order to obtain rotor resistance estimate, any on-line rotor resistance estimator can be used if the actual rotor resistance is precisely predicted, such as in [11-18].

References

[1] M. N. Uddin, Sang Woo Nam, "New Online Loss-Minimization-Based Control of an Induction Motor Drive," *IEEE transactions on Power Electronics*, vol. 23, pp. 926-933, March 2008.
DOI: https://doi.org/10.1109/TPEL.2007.915029

[2] Y. Wang, J. Arribas, T. Ito, and R. Lorenz, "Loss Manipulation Capabilities of Deadbeat Direct Torque and Flux Control Induction Motor Drives," *IEEE transactions on Industry Applications*, vol. 51, no. 6, pp. 4554-4566, 2015.
DOI: https://doi.org/10.1109/TIA.2015.2455030

[3] S. Odhano, R. Bojoi, A. Boglietti, S. Rosu, and G. Griva, "Maximum Efficiency per Torque Direct Flux Vector Control of Induction Motor Drives," *IEEE Transactions on Industry Applications,* vol. 51, no. 6, pp. 4415 – 4424, 2015.
DOI: https://doi.org/10.1109/TIA.2015.2448682

[4] O. S. Ebrahim, M. A. Badr, A. S. Elgendy, P. K. Jain, " ANN-Based Optimal Energy Control of Induction Motor Drive in Pumping," *IEEE transactions on Energy Conversion*, vol. 25, no. 3, pp. 652-660, 2010.
DOI: https://doi.org/10.1109/TEC.2010.2041352

[5] Y. Liu and A. Bazzi, "A Comprehensive Analytical Power Loss Model of an Induction Motor Drive System with Loss Minimization Control," *2015 IEEE International Electric Machines & Drives Conference (IEMDC),* pp. 1638-1643, May 2015.

[6] S. Gennaro, J. Dominguez, and M. Meza, "Sensorless High Order Sliding Mode Control of Induction Motors with Core Loss," *IEEE Transactions on Industrial Electronics*, vol. 61, no. 6, pp. 2678- 2689, 2014.
DOI: https://doi.org/10.1109/TIE.2013.2276311

[7] M. Farasat, A. Trzynadlowski, and M. Fadali, " Efficiency Improved Sensorless Control Scheme for Electric Vehicle Induction Motors," *IET Electrical Systems in Transportation*, pp. 122-131, December 2014.

[8] C. Kwon, S. D. Sudhoff, "Genetic Algorithm-based Induction Machine Characterization Procedure with Application to Maximum Torque Per Amp Control," *IEEE Transactions on Energy Conversion*, vol. 21, pp. 405-415, 2006.
DOI: https://doi.org/10.1109/TEC.2006.874224

[9] O. Wasynczuk, S.D. Sudhoff, K.A. Corzine, J.L. Tichenor, P.C. Krause, I.G. Hansen, and L.M. Taylor, "A Maximum Torque Per Ampere Control Strategy for Induction Motor Drives," *IEEE Transactions on Energy Conversion*, vol. 13, no. 2, pp. 163-169, June 1998.
DOI: https://doi.org/10.1109/60.678980

[10] S. D. Sudhoff, D. C. Aliprantis, B. T. Kuhn , and P. L. Chapman, "An Induction Machine Model for Predicting Inverter – Machine Interaction," *IEEE Transactions on Energy Conversion*, vol. 17, pp. 203-210, June 2002.
DOI: https://doi.org/10.1109/TEC.2002.1009469

[11] T. A. Najafabadi, F. R. Salmasi, P. Jabehdar-Maralani, "Detection and Isolation of Speed-, DC-Link Voltage-, and Current-Sensor Faults Based on an Adaptive Observer in Induction-Motor," *IEEE Transaction on industrial electronics*, vol. 58, no. 5, pp. 1662-1672, 2011.
DOI: https://doi.org/10.1109/TIE.2010.2055775

[12] T. Orlowska-Kowalska, M. Dybkowski, "Stator-Current-Based MRAS Estimator for a Wide Range Speed-Sensorless Induction-Motor," *IEEE Transaction on industrial electronics*, vol. 57, no. 4, pp. 1296-1308, 2010.
DOI: https://doi.org/10.1109/TIE.2009.2031134

[13] C. Kwon, S. D. Sudhoff, "An On-line Rotor Resistance Estimator for Induction Machine Drives ," *the 2005 International Electric Machines and Drives Conference*, pp. 391-397, May 2005.

[14] M. Barut, R. Demir, E. Zerdali, R. Inan, "Real-Time Implementation of Bi Input-Extended Kalman

Filter-Based Estimator for Speed-Sensorless Control of Induction Motors," *IEEE transactions on Industrial Electronics,* vol. 59, pp. 4197-4206, 2012.
DOI: https://doi.org/10.1109/TIE.2011.2178209

[15] L. Amezquita-Brooks, J. Liceaga-Castro, E. Liceaga-Castro, "Speed and Position Controllers Using Indirect Field Oriented Control: A Classical Control Approach," *IEEE transactions on Industrial Electronics*, vol. 61, no. 4, pp. 1928-1943, 2013.
DOI: https://doi.org/10.1109/TIE.2013.2262750

[16] M.S. Zaky, "Stability Analysis of Speed and Stator Resistance Estimators for Sensorless Induction Motor Drives," *IEEE transactions on Industrial Electronics,* vol. 59, pp. 858-870, 2013.
DOI: https://doi.org/10.1109/TIE.2011.2161658

[17] M. Angulo and R. Carrillo-Serrano, "Estimating Rotor Parameters in Induction Motors using High-order Sliding Mode Algorithms," *IET Control Theory & Applications*, vol. 9, no. 4, pp. 573-578, 2015.
DOI: https://doi.org/10.1049/iet-cta.2014.0110

[18] J. Kan, K. Zhang, and Z. Wang, "Indirect Vector Control with Simplified Rotor Resistance Adaptation for Induction Machine," *IET Power Electronics*, vol. 8, no. 7, pp. 1284-1294, 2015.
DOI: https://doi.org/10.1049/iet-pel.2014.0422

[19] P. C. Krause, O. Wasynczuk, S. D. Sudhoff, Analysis of Electric Machinery and Drive Systems, IEEE Press, 2002.
DOI: https://doi.org/10.1109/9780470544167

[20] "Energy Systems Analysis Consortium (ESAC) Genetic Optimization System Engineering Tool (GOSET) Ver 1.02 ," School of Electrical and Computer Engr., Purdue Univ., West Lafayette, IN, 47907, 2003.

[21] J. Kim, J. Choi, and S. Sul, "Novel Rotor Flux Observer Using Observer Characteristic Function in Complex Vector Space for Field Oriented Induction Motor Drives," *IEEE transactions on Industry Applications*, vol. 38, pp. 1334-1443, Sep/Oct 2002.
DOI: https://doi.org/10.1109/TIA.2002.802994

[22] P. L. Jansen and R. D. Lorenz, "A Physically Insightful Approach to the Design and Accuracy Assessment of Flux Observer for Field Oriented Induction Machine Drives," *IEEE Transactions on Industry Applications*, vol. 30, no. 1, pp. 101-110. Jan/Feb 1994.
DOI: https://doi.org/10.1109/28.273627

Chun-Ki Kwon [Regular member]

- Feb. 1994 : Korea Univ., Electrical Engineering, ME
- Aug. 2005 : Purdue Univ., Electrical Engineering, PhD
- Mar. 2008 ~ current : Soonchunhyang Univ., Dept. of Medical IT Engineering, Associate Professor

<Research Interests>
Bio-signal processing, Medical Electric Machine

Yong-Hae Kong [Regular member]

- May 1986 : New York Univ., Computer Science, ME
- May 1990 : New York Univ., Computer Science, PhD
- Mar. 1991 ~ current : Soonchunhyang Univ., Dept. of Medical IT Engineering, Professor

<Research Interests>
Hospital Information, Intelligent Web